

## Flexible Photovoltaics/Fuel Cell/Wind Turbine (PVFCWT) Hybrid Power System Designs

Meng-Han Lin, Vincentius Surya Kurnia Adi, Chuei-Tin Chang\*

National Cheng Kung University, Tainan 70101, Taiwan (R. O. C.)  
 ctchang@mail.ncku.edu.tw

Extensive studies have been performed in the past to integrate more than one 'green' energy source, e.g., solar, wind and hydrogen, for power generation. For actual operation in a realistic environment, such a hybrid process must be fully functional despite random fluctuations in energy supplies and power demands. A common option for accommodating the uncertain disturbances and their cumulative effects is to introduce battery into a properly structured system. However, by using an ad hoc approach, these schemes may be either overdesigned or inoperable. A generic mathematical programming model is thus adopted in the present study to compute a so-called temporal flexibility index for use as a performance measure. In order to demonstrate the usefulness of this assessment criterion, a large collection of photovoltaics/fuel cell/wind turbine (PVFCWT) systems were configured for a specific application and then compared accordingly so as to identify the best combination of energy supplies. A MATLAB/Simulink simulation program has also been developed in this work to validate these design decisions.

### 1. Introduction

Renewable energy sources, such as solar, wind, biomass, etc., are attracting more and more attention in recent years for use as the alternatives of fossil fuels. Among them, the photovoltaic (PV) generator that directly converts solar energy into electricity has been widely utilised in low power applications. It is widely regarded as unsuitable for off-grid applications due to the uncertain nature of solar irradiation. One method to overcome this problem is to integrate the PV generator with other energy sources e.g., fuel cell (FC) and wind turbine (WT). The fuel cell can be a good candidate for this purpose since it is blessed with high efficiency and quick response, while the wind turbines are usually connected into some form of electrical network so as to satisfy the overall power demand partially. Their feasibility in coordination with a PV system has been successfully demonstrated in both grid-connected and stand-alone applications.

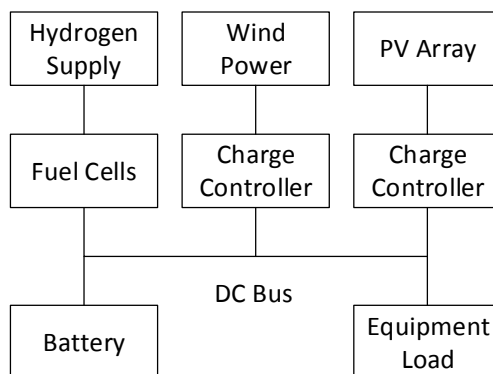


Figure 1: PVFCWT power generation system (adapted from Saathoff, 2009)

Although numerous studies on the optimisation, modelling and design of the photovoltaics/fuel cell (PVFC) and the PVFCWT hybrid systems have been carried out in recent years, e.g., see Wang and Nehrir (2008), where overall power management strategy of PVFCWT hybrid system is addressed, Saathoff (2009), where the importance of solar, wind, fuel cell, and batteries are discussed, and Chen et al. (2013) where a mathematical programming approach is established for the analysis and design of the off-grid hybrid power system (HPS). It is worth noting that most of them did not consider the important issues concerning operational flexibility. The incorporation of a large enough battery can obviously facilitate smooth operation, yet it is still important to optimally allocate the capacities of various different units in the hybrid system (see Figure 1) so as to avoid overdesign. For this purpose, the system flexibility must be evaluated rigorously with a quantitative measure.

In a previous study, Adi and Chang (2013) developed a generic mathematical program to compute a so-called temporal flexibility index for quantifying the system's ability to buffer the accumulated changes in process parameters. These authors later applied the same analysis in evaluating and designing the PVFC systems (Adi and Chang, 2015). Therefore, temporal flexibility analysis of the PVFCWT system is deemed useful for identifying realistic designs.

The rest of the paper is organised as follows. The mathematical models of basic components in the PVFCWT system are first presented in the next section. In Section 3, the novel concept of temporal flexibility is outlined and a generic programming formulation for computing temporal flexibility is also given. A series of case studies have been performed to validate the proposed design approach in this work. The optimisation and simulation results are thoroughly analysed and discussed in Section 4. Finally, conclusions are drawn in Section 5.

## 2. Unit Models

As shown in Figure 1, four basic components are considered in this analysis, i.e., solar cell, polymer electrolyte membrane (PEM) fuel cell, wind turbine, and battery. The mathematical models of these essential units are shown below:

### 2.1 Photovoltaic Cell

A solar module typically consists of several cells connected in series. The conventional modelling approach is to describe the p-n junction physics in the form of equivalent circuits. For example, the cell current  $I_{PV}$  is determined as the follows:

$$I_{PV} = I_{ph} - I_{d1} - I_{d2} - I_p \quad (1)$$

where,  $I_{ph}$  denotes the light-generated current (which is a function of solar radiation and cell temperature);  $I_{d1}$  denotes the diffusion current from the base to emitter layers;  $I_{d2}$  represents the effect of the generation and re-combination current in the junction space charge region;  $I_p$  represents the current flowing through the shunt resistance. Due to space limitation, detailed descriptions of additional formulations are omitted in this paper. A complete version can be found in Shen et al. (2011).

### 2.2 Fuel Cell

The actual voltage  $U_{FC}$  is lower than the open-circuit voltage  $U_{OCV}$  in an operating fuel cell due to various irreversible loss mechanisms. These losses are originated from three main sources due to activation overpotential  $\eta_{act}$ , concentration overpotential  $\eta_{conc}$ , and Ohmic overpotential  $\eta_{ohm}$ . The actual cell voltage should be represented as follows:

$$U_{FC} = U_{OCV} - \eta_{act} - \eta_{conc} - \eta_{ohm} \quad (2)$$

For the sake of brevity, the explicit formulas for computing the right side of Eq(2) are not included here. For the actual calculation carried out in this study, they were obtained from Hwang et al. (2009).

### 2.3 Wind Turbine

The power  $P_{WT}$  (in W) extracted from wind can be expressed as

$$P_{WT} = \frac{1}{2} \rho C_p(\lambda, \beta) A_2 c_x^3 \quad (3)$$

where,  $\rho$  is the air density in kg/m<sup>3</sup>,  $A_2$  is the disc area swept by the rotor blades in m<sup>2</sup>, and  $c_x$  is the wind velocity in m/s.  $C_p$  is called the power coefficient or the rotor efficiency and is a function of tip speed

ratio (TSR or  $\lambda$ ) and pitch angle ( $\vartheta$ ) (Heier, 1998). It is worth noting that wind turbine can produce power within the cut-in and cut-out wind speed range, i.e., lower and upper operating wind speed limit. Since the detailed model formulations are available elsewhere (Dixon and Hall, 2014), they are all excluded so as to shorten the paper.

## 2.4 Battery

The discharge model of Li-ion battery is adopted from the work of Tremblay and Dessaint (2009) which accurately characterises the voltage dynamics when the current varies. Specifically, the battery voltage is given by:

$$V_{batt} = E_0 - \underbrace{K \frac{Q}{Q-it}}_{\text{Pol. voltage}} it - R \times I_{batt} + A \exp(-B \times it) - \underbrace{K \frac{Q}{Q-it}}_{\text{Pol. resistance}} I_{batt}^* \quad (4)$$

where,  $V_{batt}$  is the battery voltage,  $E_0$  is the battery constant voltage,  $K$  is the polarisation constant or polarisation resistance,  $Q$  is the battery capacity,  $it = \int I_{batt} dt$  is the actual battery charge,  $A$  is the exponential zone amplitude,  $B$  is the exponential zone time constant inverse,  $R$  is the internal resistance,  $I_{batt}$  is the battery current,  $I_{batt}^*$  is the filtered current. Further details can be found in Tremblay and Dessaint (2009).

## 3. Temporal Flexibility Index

Dimitriadis and Pistikopoulos (1995) replaced the equality constraints in the conventional model formulations for steady-state flexibility analysis with a system of differential-algebraic equations, i.e.

$$f_i(\mathbf{d}, \mathbf{z}(t), \mathbf{x}(t), \dot{\mathbf{x}}(t), \boldsymbol{\theta}(t)) = 0 \quad (5)$$

where,  $t \in [0, H]$  and  $\mathbf{x}(0) = \mathbf{x}^0$ . The dynamic flexibility index can be computed accordingly with the following model:

$$FI_d = \max \delta \quad (6)$$

subject to Eq(5) and

$$\max_{\boldsymbol{\theta}(t)} \min_{\mathbf{z}(t)} \max_{j,t} g_j(\mathbf{d}, \mathbf{z}(t), \mathbf{x}(t), \boldsymbol{\theta}(t), t) \leq 0 \quad (7)$$

$$\boldsymbol{\theta}^N(t) - \delta \Delta \boldsymbol{\theta}^-(t) \leq \boldsymbol{\theta}(t) \leq \boldsymbol{\theta}^N(t) + \delta \Delta \boldsymbol{\theta}^+(t) \quad (8)$$

where,  $f_i$  is the  $i^{th}$  equality constraint in the design model (e.g. the mass or energy balance equation for a processing unit);  $g_j$  is the  $j^{th}$  inequality constraint (e.g. a capacity limit);  $\mathbf{d}$  represents a vector which contains the design variables corresponding to the structure and equipment sizes of the plant;  $\mathbf{z}$  denotes a vector which contains the control variables that can be adjusted during operation, e.g. flows and utility loads;  $\mathbf{x}$  is a vector which contains the state variables that define the system, e.g. concentrations, temperatures and voltages;  $\boldsymbol{\theta}$  denotes the vector which contains the uncertain parameters, e.g. solar irradiation rate and wind speed.

To facilitate the proposed temporal flexibility analysis in the present study, let us assume that the cumulative effects of uncertain disturbances can be assessed by replacing Eq(8) with

$$\boldsymbol{\theta}^N(t) - \Delta \boldsymbol{\theta}^-(t) \leq \boldsymbol{\theta}(t) \leq \boldsymbol{\theta}^N(t) + \Delta \boldsymbol{\theta}^+(t) \quad (8')$$

and

$$-\delta \Delta \boldsymbol{\theta}^- \leq \int_0^H (\boldsymbol{\theta}(\tau) - \boldsymbol{\theta}(\tau)^N) d\tau \leq +\delta \Delta \boldsymbol{\theta}^+ \quad (9)$$

where the anticipated values of accumulated deviations ( $\Delta \boldsymbol{\theta}^-$  and  $\Delta \boldsymbol{\theta}^+$ ) should be extracted independently from historical data. A mathematical programming model can then be established to determine the temporal flexibility index  $FI_t$  by maximising the scalar variable  $\delta$  (Adi and Chang, 2012). The specific computation procedure is outlined in Adi and Chang (2013).

#### 4. Case Studies

The case studies presented below are adopted mainly to demonstrate the important role of flexibility analysis in evaluating and synthesising operable designs. The model parameters of solar module were taken from Shen et al. (2011) and fuel cell were taken from Hwang et al. (2009) while those of wind turbine were from Dixon and Hall (2014). The battery parameters were extracted from the Simscape block of MATLAB/Simulink. Based on the assumption that all components are interconnected via an electrical bus, the charging/discharging behaviour of battery can be described as follows:

$$\frac{dit}{dt} = I_{batt} = I_{PV} + I_{FC} + I_{WT} - I_{demand} \quad (10)$$

A total of four uncertain parameters were considered in all cases, i.e., the output powers from the PV, FC and WT units, respectively, and also the power demand. The chosen nominal profiles of solar irradiation rate and wind speed can be found in Figure 2(a), while the nominal hydrogen flowrate is set to be a constant at 0.09 kmol/h. On the basis of Eq(8'), it is assumed that each parameter may vary between  $\pm 20\%$  of the nominal level at any time. The anticipated values of  $\Delta\Theta^-$  and  $\Delta\Theta^+$  for each module are predetermined by integrating the lower and upper limits of the corresponding output power. For illustration purpose, a preliminary design has been analysed for 3 PV modules (5 parallel 400-series cells – rated at 8.5 kW/module), 1 FC module (65 cells – rated at 7.4 kW/module), 6 WT modules (rated at 7 kW/module) and a battery (2,568 Ah, 50 % initial SOC). Based on these specifications, the nominal profile of total power supply in Figure 2(a) can be produced via numerical simulation with MATLAB/Simulink. On the other hand, the nominal profile of power demand of a remote village (Mishra and Singh, 2013) has been adopted in all cases reported here (see Figure 2(b)), from which 20 % positive and negative deviations are anticipated. The corresponding nominal SOC profile of the battery is also shown in Figure 2(b). At 2,568 Ah, the fully charged battery can withstand up to about 10 h of the average load without recharging.

As a design variable, an energy supply-to-demand ratio should be specified a priori, i.e.

$$r_{SD} = \frac{\text{Nominal daily energy supply}}{\text{Nominal daily energy demand}} \quad (11)$$

The denominator of this ratio can be computed by numerically integrating the power demand profile in Figure 2(a) over a period of 24 h, while the numerator was computed according to the following formula

$$\text{Nominal daily energy supply} = E_{PV}^N \times N_{PV} + E_{FC}^N \times N_{FC} + E_{WT}^N \times N_{WT} + E_B^I \times N_B \quad (12)$$

where,  $E_{PV}^N$ ,  $E_{FC}^N$ ,  $E_{WT}^N$  denote the nominal daily energy supply of PV, FC, and WT modules, respectively, and they can be determined by integrating the nominal profiles of the output powers produced by the corresponding modules with MATLAB/Simulink;  $E_B^I$  denotes the initial energy stored in the battery, which can be treated as a design specification.

For the purpose of evaluating economic performance, the installation cost of every component in the hybrid system was estimated according to literature data. Based on the unit cost reported in Dovetail (2015), i.e. 4 \$/W, the figure \$ 34,000 was adopted as the approximate cost of an 8.5 kW PV module. It was also assumed that a 7.5 kW Ene-Farm FC system (by Tokyo Gas and Panasonic) could be purchased with \$ 226,000 (FuelCellToday, 2015). The installation cost of a WT module was estimated to be \$ 14,000 / 7 kW based on the reported value of 2,000 \$/kW (IER, 2015). Finally, a preliminary estimate of \$ 17,348 was used as the capital cost of a 2,568-Ah battery bank (Wholesale Solar, 2015).

The values of  $FI_t$  for different supply-to-demand ratios were computed by solving the proposed model according to the same initial SOC for battery bank (50 %). The results are summarized in Table 1. It should be noted first that, since a feasible operation requires  $r_{SD} > 100\%$ , the flexibility index in Case 1 naturally falls below the target value of 1. As expected, the operational flexibility of a hybrid power generation system can in general be improved by raising  $r_{SD}$ . Note that, despite the high installation cost of FC system, the operational flexibility of hybrid system can be greatly enhanced since it is a stable power source. On the other hand, since the sun light and wind are expected to be both strong during the day, the power produced by PV and WT modules should be more than enough for day-time consumption despite random fluctuations. This excess energy should be stored in the battery and used later to satisfy the anticipated evening demand. Although as mentioned before a low  $r_{SD}$  usually fails to meet this need, i.e.

$FI_t < 1$ , the power produced by PV and/or WT modules may be wasted when an exceedingly large ratio is

adopted. This is because of the fact that, in the latter case, the stored energy in battery may reach the maximum tolerable limit. For example, as shown in Figure 2(b), the excess energy cannot be charged to the battery during the period from around 12 h to 18 h.

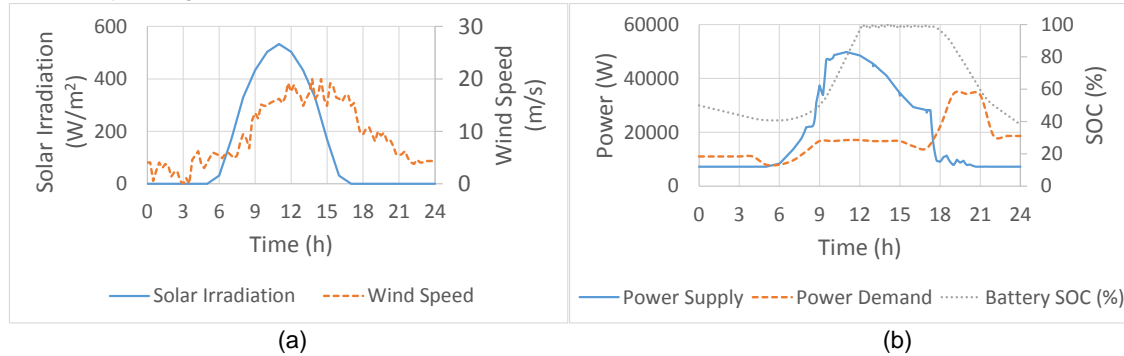


Figure 2: (a) Nominal profile of solar irradiation rate and wind speed; (b) Nominal profiles of total power supply vs power demand and battery SOC profile

Table 1: Flexibility indices of hybrid power generation systems

Case	$N_{PV}$	$N_{FC}$	$N_{WT}$	$N_B$	$\phi_{PV}$	$\phi_{FC}$	$\phi_{WT}$	$\phi_B$	$r_{SD}$	$FI_t$	Cost
1	6	1	3	1	21.94 %	31.86 %	21.00 %	25.20 %	99.2 %	0.822	\$ 489,348
2	8	1	3	1	27.24 %	29.68 %	19.61 %	23.47 %	106.5 %	1.255	\$ 557,348
3	6	1	4	1	20.47 %	29.73 %	26.28 %	23.52 %	106.3 %	1.228	\$ 503,348
4	2	1	6	1	6.88 %	29.92 %	39.53 %	23.67 %	105.6 %	1.178	\$ 395,348
5	2	1	6	2	5.56 %	24.20 %	31.97 %	38.28 %	130.7 %	2.559	\$ 412,696
6	2	1	3	2	6.62 %	28.80 %	19.02 %	45.56 %	109.8 %	1.069	\$ 370,696

It can also be observed from Table 1 that, in terms of flexibility enhancement, the contribution of WT is relatively less significant than that of PV generator. This is due to the narrower operating range imposed by the cut-in and cut-out wind speed in the former case. Still, WT is an attractive candidate since it is relatively inexpensive, i.e. \$ 14,000 / 7 kW WT module vs \$ 34,000 / 8.5 kW PV module.

More specific observations can be summarised below:

- In Case 1, a preliminary structure with 6 PV modules, 1 FC module, 3 WT modules and a 2,568 Ah battery is evaluated with corresponding  $\phi_{PV}$ ,  $\phi_{FC}$ , and  $\phi_{WT}$  to be 21.94 %, 31.86 %, and 21.00 %, respectively, and the total  $r_{SD}$  is below 100 % (99.2 %). This configuration was chosen to evenly distribute all energy sources. Such a simple strategy results in an inflexible system design ( $FI_t < 1$ ).
- By comparing Cases 1 and 2, one can see that  $FI_t$  can be drastically raised from 0.822 to 1.255 by increasing  $N_{PV}$  from 6 to 8 and the corresponding cost is increased 13.9 % from \$ 489,348 to \$ 557,348. On the other hand, by adding a WT model (see cases 1 and 3), the system flexibility can also be enhanced to a similar degree ( $FI_t = 1.228$ ) with a lower cost burden.
- Since the installation cost of a WT module is lower than that of a PV module, one would expect that by replacing a few former units with latter can achieve similar improvement in operational flexibility at a lower cost. This is shown in Case 4 when  $N_{PV}$  is reduced to 2 and  $N_{WT}$  increased to 6. Indeed, the resulting  $FI_t$  is roughly the same (1.178) while the installation cost is lower (i.e., \$ 395,348 at 19.2 % cost saving).
- Note that the battery plays a critical role in improving system flexibility. As shown in Figure 3(a), at around 17 h, only the FC module is capable of producing power online and the energy stored in battery must be utilised to make up the power shortage. Since the capital costs of battery and WT module are roughly in the same range, it may be worthwhile to introduce extra battery capacity. As observed from Cases 4 and 5, increasing the battery number can improve  $FI_t$  from 1.178 to 2.559. Since the  $FI_t$  in Case 5 is quite large, one may remove a few PV or WT modules so that  $FI_t$  is near and above the target value of 1. As shown in Case 6, the  $FI_t$  reaches 1.069 and the corresponding installation cost is \$ 370,696 (24.2 % saving cost). Interestingly, the value of  $r_{SD}$  in this case is higher

and  $FI_t$  is lower than the ones determined in Cases 2 - 4. Also note that  $\phi_B$  is larger in Case 6 and the total active power supplies PV, FC, and WT is lower when compared with the above three cases. This extra storage space can be fully utilized to avoid wasting the excess energy generated by the PV and WT modules during the day. Since the installation cost of Case 6 is the lowest with  $FI_t > 1$ , it is therefore recommended for the present design problem.

## 5. Conclusions

In the present study, the temporal flexibility analysis has been successfully applied to design a flexible hybrid power generation system according to any given time-variant demand profile with uncertain disturbances. For this purpose, the overall energy supply-to-demand ratio ( $r_{sd}$ ) clearly must be targeted at a larger-than-one value to ensure operational feasibility. The corresponding power demand at any instance is supposed to be satisfied as much as possible with the instantaneous outputs of PV, FC and WT modules, while the rates of energy inputs to these units, i.e. solar irradiation rate, hydrogen feed rate and wind speed, are considered to be uncertain and time dependent. Any discrepancy between supply and demand during operation can only be buffered with battery. Therefore, a flexible system configuration should be synthesised by properly allocating capacities of the three different types of power-generating components and, also, optimally sizing the battery and setting its initial charge level. Two performance measures, i.e. the flexibility index and the total capital cost, are adopted in the present work to facilitate making these decisions systematically. The effectiveness of such a design strategy has been demonstrated in the case studies.

## References

- Adi V.S.K., Chang C.T., 2012, Dynamic flexibility analysis with differential quadratures, *Comput. Aid. Chem. Eng.*, 31, 260 – 264.
- Adi V.S.K., Chang C.T., 2013, A mathematical programming formulation for temporal flexibility analysis, *Comput. Chem. Eng.* 57, 151–158.
- Adi V.S.K., Chang C.T., 2015, Development of flexible designs for PVFC hybrid power systems, *Renew. Energ.* 74, 176–186.
- Chen C.L., Lai C.T., Lee J.Y., 2013, A process integration technique for targeting and design of off-grid hybrid power networks, *Chemical Engineering Transactions*, 35, 499–504.
- Dimitriadis V.D., Pistikopoulos E.N., 1995, Flexibility analysis of dynamic systems, *Ind. Eng. Chem. Res.* 34, 4451–4462.
- Dixon S.L., Hall C.A., 2014, *Fluid Mechanics and Thermodynamics of Turbomachinery* (7th Ed.), Chap. 10 – Wind Turbines, Butterworth-Heinemann, Oxford, UK.
- Dovetail, 2015, Pricing for solar photovoltaic (PV) systems, <[www.dovetailsolar.com](http://www.dovetailsolar.com)> accessed 09.02.2015.
- FuelCellToday, 2015, Tokyo Gas and Panasonic launch smaller, more efficient and cheaper Ene-Farm residential fuel cell, <[www.fuelcelltoday.com](http://www.fuelcelltoday.com)> accessed 09.02.2015.
- Heier S., 1998, *Grid Integration of Wind Energy Conversion Systems*, Wiley, New York, USA.
- Hwang J.J., Lai L.K., Wu W., Chang W.R., 2009, Dynamic modeling of a photovoltaic hydrogen fuel cell hybrid system, *Int. J. Hydrogen Energ.*, 34, 9531–9542.
- IER (Institute for Energy Research), 2015, The hidden costs of wind power <[instituteforenergyresearch.org](http://instituteforenergyresearch.org)> accessed 09.02.2015.
- Mishra R., Singh S., 2013, Sustainable energy plan for a village in Punjab for self energy generation, *Int'l J. Renew. Energ. Res.* 3, 640–646.
- Saathoff S., 2009, Hybrid power is the new green <[www.ospmag.com](http://www.ospmag.com)> accessed 09.02.2015.
- Shen W.X., Choo F.H., Wang P., Loh P.C., Khoo S.Y., 2011, Development of a mathematical model for solar module in photovoltaic systems, 2011 6<sup>th</sup> ICIEA, Beijing, China, 2056-2061.
- Tremblay O., Dessaint L.-A., 2009, Experimental validation of a battery dynamic model for EV applications, *World Electr. Veh. J.*, 3, 1–10.
- Wang C., Nehrir M.H., 2008, Power management of a stand-alone wind/photovoltaic/fuel cell energy system, *IEEE T Energy Conver*, 23, 957–967.
- Wholesale Solar, 2015, Rolls battery engineering <[www.wholesalesolar.com](http://www.wholesalesolar.com)> accessed 09.02.2015.